Journal of Alloys and Compounds 480 (2009) 889–892

Contents lists available at ScienceDirect

Journal of Alloys and Compounds

journal homepage: www.elsevier.com/locate/jallcom

Preparation of high-quality $BiFeO_3$ nanopowders via a polyacrylamide gel route

T. Xian [b], H. Yang [a,b,*], X. Shen [b], J.L. Jiang [b], Z.Q. Wei [b], W.J. Feng [b]

[a] State Key Laboratory of Gansu Advanced Non-ferrous Metal Materials, Lanzhou University of Technology, Lanzhou 730050, People's Republic of China
[b] School of Science, Lanzhou University of Technology, Lanzhou 730050, People's Republic of China

ARTICLE INFO

Article history:
Received 17 December 2008
Received in revised form 17 February 2009
Accepted 19 February 2009
Available online 4 March 2009

PACS:
75.80.+q
81.07.−b
81.20.Fw

Keywords:
$BiFeO_3$
Nanoparticles
Polyacrylamide gel

ABSTRACT

We report here an acrylamide gel route to prepare $BiFeO_3$ nanopowder. In this route, the gelation of the solution is achieved by the formation of a polymer network: the polyacrylamide, which provides a structural framework for the growth of particles. It is demonstrated that pure $BiFeO_3$ phase can be obtained using EDTA as the chelating agent. In addition, we find when the used acrylamide is 9 times the amount (in mole) of the cations and an appropriate amount of glucose is added to the precursor solution, the particle morphology can be much improved. SEM observations reveal that the powder prepared under the optimal conditions has a small and uniform particle size, and the particles are almost spherical and polydisperse without any agglomeration or adhesion. DSC measurements identify the presence of the two ferroic phase transitions in our product, i.e., the antiferromagnetic transition at ~370 °C and the ferroelectric transition at ~830 °C.

1. Introduction

Bismuth ferrite ($BiFeO_3$) with a perovskite-type structure has been extensively studied as a multiferroic material during recent years. It is well established that $BiFeO_3$ is antiferromagnetic with the Néel temperature $T_N \approx 370$ °C and ferroelectric with the Curie temperature $T_C \approx 830$ °C [1–3]. Due to its high Néel temperature and high Curie temperature, $BiFeO_3$ is regarded to be an excellent candidate for multiferroic applications. However, the effective incorporation of this multiferroic oxide into practical devices has been hindered due to leakage current problems resulting likely from defects and nonstoichiometry. Doping [4] and preparation of high-quality samples [5] have been generally considered to improve the electrical properties of $BiFeO_3$.

The creation of nanostructures also offers great potential to tailor and/or enhance the physical properties. For example, epitaxial $BiFeO_3$ thin films have shown an enhancement in ferroelectric polarization and related properties, which makes an opportunity to create film-based magnetoelectric devices [6]. Nanosized $BiFeO_3$ powders have been reported to exhibit weak ferromagnetism at room temperature, which is different from the magnetic property of bulk samples [7,8]. Furthermore, $BiFeO_3$ nanopowders have shown the prominent visible-light photocatalytic activity that is ascribed to the small bandgap and the high surface area of nanosized $BiFeO_3$ [8,9]. These nanosize-induced properties are expected to widen the potential applications of $BiFeO_3$.

Various wet chemical routes have been used to prepare $BiFeO_3$ nanopowders, such as hydrothermal synthesis [10], co-precipitation [11], microemulsion technique [12], combustion synthesis [13], ferrioxalate precursor method [14], and sol–gel process [15–17]. Among these methods, the sol–gel route is very attractive, having the main advantage of easy control of chemical composition. Up to now, in the sol–gel synthesis of $BiFeO_3$ powders, the gel is built up by chemical and physical bonds between the chemical species. We report here a polyacrylamide gel route to prepare $BiFeO_3$ nanopowder. In this route, the solution containing the required cations is gelled by using acrylamide; during the gelation process, acrylamide is polymerized to form a polymer network, which provides a structural framework for the growth of particles. We have demonstrated that this gel route allows the production of high-quality $BiFeO_3$ nanopowder with uniform particle size and in spherical shape.

2. Experimental

The synthesis process of $BiFeO_3$ nanopowder via the polyacrylamide gel method is described as follows. In terms of the atomic ratio Bi:Fe = 1:1, stoichiometric amounts of $Bi(NO_3)_3 \cdot 5H_2O$ and $Fe(NO_3)_3 \cdot 9H_2O$ were dissolved in an aqueous solution of nitric acid (1.6 mol/L). After the solution was clear and without residue, a stoichiometric amount of ethylenediamine-tetraacetic acid (EDTA) (or citric acid), which was used as the chelating agent to complex the cations, was added to the

* Corresponding author at: State Key Laboratory of Gansu Advanced Non-ferrous Metal Materials, Lanzhou University of Technology, Lanzhou 730050, People's Republic of China. Tel.: +86 931 2973783; fax: +86 931 2976040.
E-mail address: hyang@lut.cn (H. Yang).

0925-8388/$ – see front matter © 2009 Elsevier B.V. All rights reserved.
doi:10.1016/j.jallcom.2009.02.068

solution in the molar ratio 1.5:1 respect to the cations. Subsequently an appropriate amount of glucose was dissolved (about 20 g in 100 ml). Finally, to the solution were added acrylamide monomers in the molar ratio 9:1 with respect to the cations, followed by adjusting the pH value to 3 by the addition of ammonia. Every step mentioned above was accompanied by constant magnetic stirring to make the solution transparent and homogeneous. The resultant solution was heated at 80 °C on a hot plate to initiate the polymerization reaction, and a few minutes later a polyacrylamide gel was formed. The gel was dried at 120 °C for 24 h in a thermostat drier. The xerogel obtained was ground into powders and then submitted to calcination at 600 °C for 3 h. At this stage the organic phase was removed, resulting in the formation of $BiFeO_3$ fine powders.

Phase purity of the powder samples was examined by X-ray diffraction (XRD) using Cu Kα radiation on a D8 Advance diffractometer. The particle morphology was investigated using a JSM-6701F field-emission scanning electron microscope (FE-SEM). Fourier transform infrared (FTIR) spectroscopy studies were carried out on a Bruker IFS 66v/S spectrometer. Thermogravimetric (TG) and differential scanning calorimetry (DSC) analyses were performed in a Netzsch STA 449C simultaneous thermal analyzer at a heating rate of 10 °C/min.

3. Results and discussion

The gelation of the solution is achieved by the formation of an organic polymer network: the polyacrylamide, which provides a structural framework to hold the precursor solution in place. There is work suggesting that the reaction of acrylamide monomers with the cation could influence the polymerization, consequently impeding formation of the gel [18]. In order to isolate the cation from the monomers, a chelating agent is generally used to complex the cation. The most commonly used chelating agents include EDTA, citric acid and oxalic acid. During the preparation of $BiFeO_3$ powder, we find that the proper choice of chelating agent can result in enhanced phase purity. Fig. 1(b) shows the XRD patterns of $BiFeO_3$ gel powder prepared using EDTA as the chelating agent and annealed at different temperatures. The xerogel dried at 120 °C is amorphous in nature. $BiFeO_3$ perovskite phase begins to form when calcined at 300 °C, and the phase formation is completed at 600 °C. No traces of impurity phases are visible in the XRD pattern

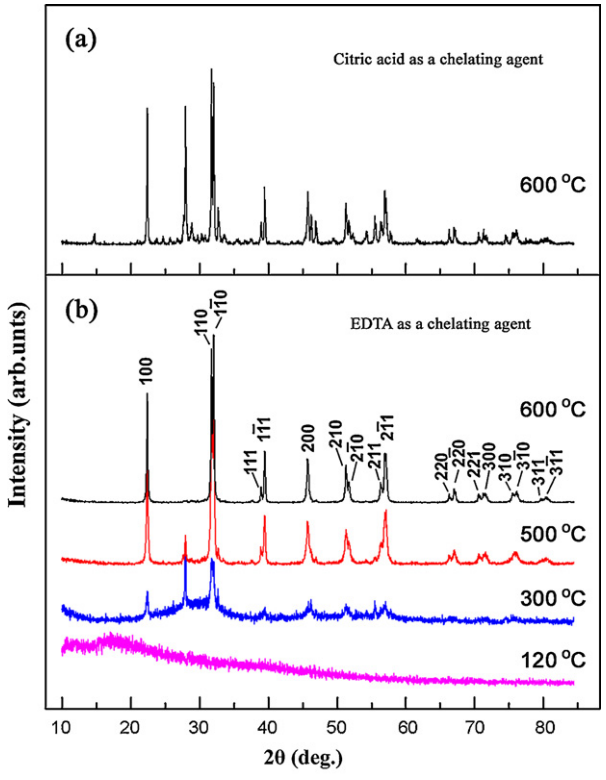

Fig. 1. XRD patterns of $BiFeO_3$ powder prepared separately using (a) citric acid and (b) EDTA as the chelating agent.

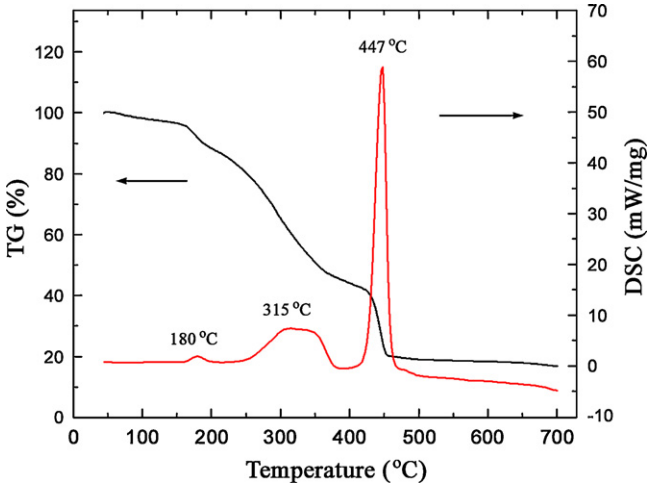

Fig. 2. TG/DSC curves of the xerogel prepared using EDTA as the chelating agent.

for the resultant $BiFeO_3$ powder. Fig. 1(a) shows the XRD pattern of $BiFeO_3$ powder (annealed at 600 °C) prepared using citric acid as the chelating agent, where additional impurity peaks including those of Bi_2O_3 and $Bi_2Fe_4O_9$ are clearly visible, indicating that the use of citric acid cannot produce a phase-pure $BiFeO_3$ product. It has been shown that citric acid forms a dimeric complex with bismuth (III) [19]. Due to the dimeric nature of the complex, the possible formation of Bi(III)–Fe(III) heteronuclear arrangement is not expected to become predominant [14]. EDTA as a chelating agent forms heterometallic polynuclear complexes in the solution, where reacting metal atoms come into close proximity [20]. Maybe this why EDTA offers the advantage over citric acid in the production of pure phase $BiFeO_3$.

Fig. 2 shows the TG/DSC curves of the xerogel, revealing three thermal decomposition steps. The exothermic reaction at ~180 °C, accompanied by the first step weight loss, is due to decomposition of anions NO_3^-. The second exothermic reaction with a large weight loss in the temperature range 270–360 °C is likely attributed to decomposition of complexes, glucose, and side-chain of polyacrylamide [21]. The last exothermic weight loss at ~447 °C is caused by decomposition of polyacrylamide's backbone and other residues [21]. No further weight loss is detected above 450 °C, indicating that the organic phase has been completely burned off. The chemical reaction is almost finished at the sintering temperature of 450 °C, resulting in the formation of $BiFeO_3$ powder; however, a higher annealing temperature is generally needed for enhancing phase purity (Fig. 1(b)).

In order to produce spherical and uniform $BiFeO_3$ particles, it is very important to prevent the gel from drastically shrinking during drying. Adding an amount of glucose to the precursor solution was shown to be able to suppress the shrinkage. This can be explained as the result of carbonization of glucose during the gel drying process. Generally the shrinkage of the gel is expected to decrease with the increase of the mass fraction of generated carbon. In addition, the quantity of used acrylamide was also revealed to have great influence on the properties of resultant $BiFeO_3$ powder. We find that when the used acrylamide is 9 times the amount (in mole) of the cations, a high-quality nanopowder of $BiFeO_3$ is allowed to be prepared. Fig. 3(a) presents the SEM micrograph of $BiFeO_3$ particles prepared under the optimal conditions, showing that the particles are almost spherical with uniform diameter around 110 nm and also the particles are polydisperse without any agglomeration. Generally too little acrylamide used in the experiment is susceptible to yield a $BiFeO_3$ powder with non-uniform particle size and in irregular shape, as seen from the SEM micrograph of Fig. 3(b) (where the

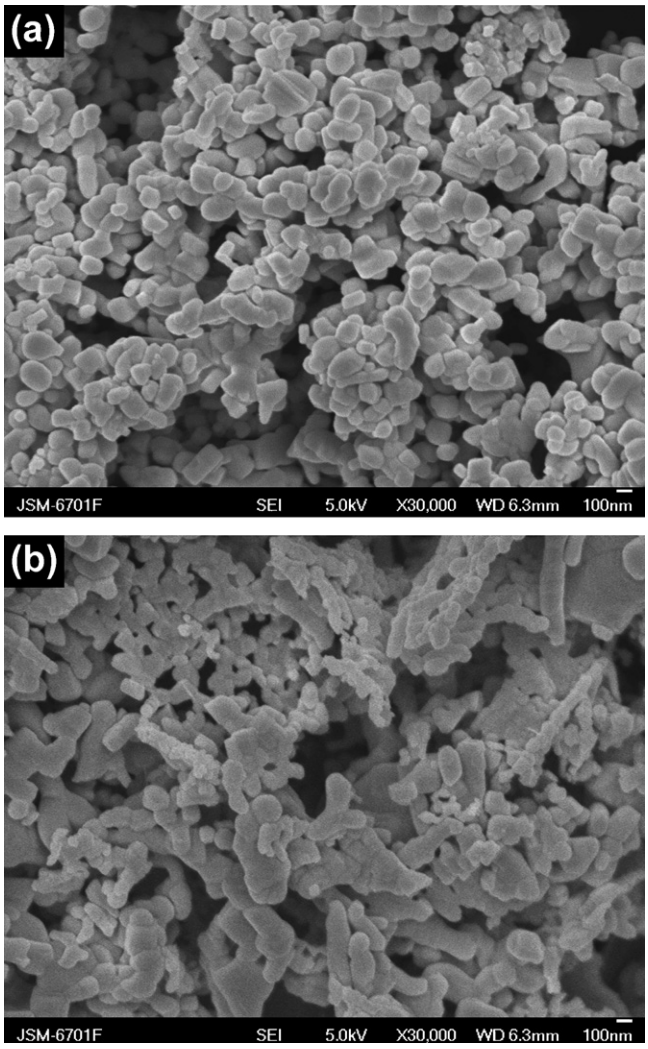

Fig. 3. SEM micrographs of $BiFeO_3$ particles prepared using different amounts of acrylamide. (a) The used acrylamide is 9 times the amount (in mole) of the cations and (b) the acrylamide is 6 times the amount of the cations.

particles were prepared when the used acrylamide is 6 times the amount of the cations).

Fig. 4(a) and (b) shows the FTIR spectra obtained, respectively, from the xerogel and the prepared $BiFeO_3$ nanopowder. In Fig. 4(a), numerous absorption peaks are visible and these peaks originate from organic phases in the xerogel. The broad absorption band in the range of 3500–3200 cm^{-1} is assigned to N–H stretching [22] which may be overlapped with O–H stretching. The peak at 2928 cm^{-1} is attributed to C–H stretching [23]. The peaks observed at 1700 and 1650 cm^{-1} are ascribed to the vibration of carboxyl groups [24]. The presence of NO_3^- is evidenced by the observation of absorption bands at 1384 and 830 cm^{-1} [25]. The band at around 1100 cm^{-1} is attributed to C–O stretching vibration [23]. In the spectrum of Fig. 4(b), all the organic peaks are seen to disappear; instead, two new absorption peaks appear at 560 and 440 cm^{-1}. The absorption features at 560 and 440 cm^{-1} are, respectively, attributed to the Fe–O stretching and bending vibrations, being characteristics of the octahedral FeO_6 groups in the perovskite compounds [26,27]. The FTIR spectroscopic results, as well as the XRD data (see Fig. 1(b)), demonstrate that pure $BiFeO_3$ phase can be obtained by calcining the xerogel at a temperature of 600 °C. Generally bismuth loss is not expected at this low synthesis temperature; however, the high temperature synthesis of $BiFeO_3$ (such as the solid-state synthesis) usually results in the evaporation loss of bismuth as well as the

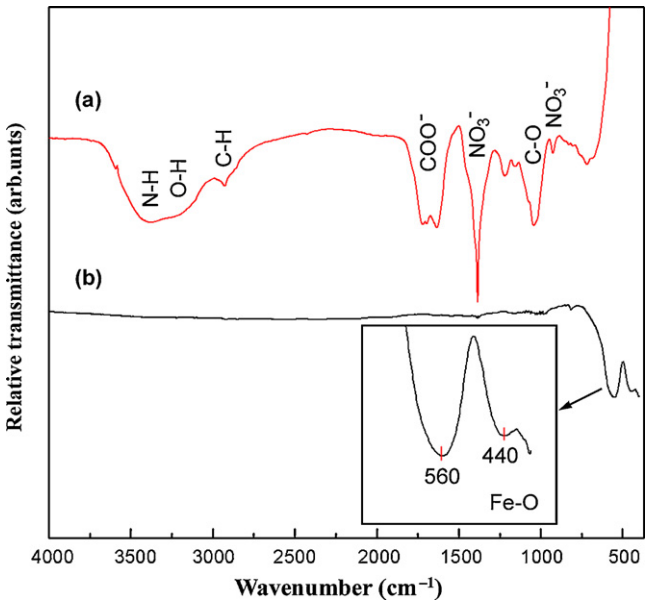

Fig. 4. FTIR spectra obtained from (a) the xerogel dried at 120 °C and (b) the $BiFeO_3$ powder produced by calcining the xerogel at 600 °C.

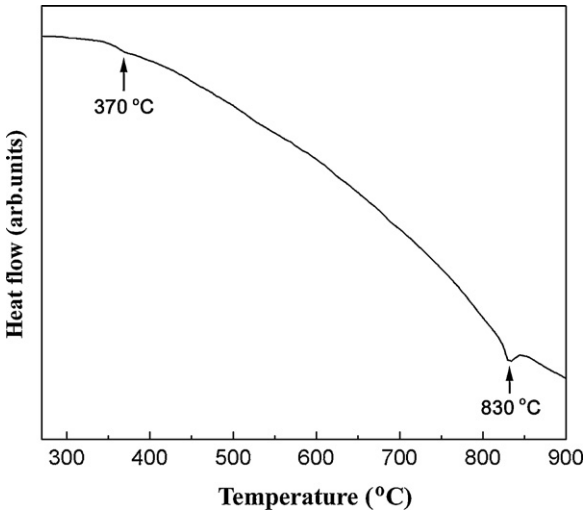

Fig. 5. DSC curve of $BiFeO_3$ nanopowder, revealing two endothermic peaks at ~370 and ~830 °C.

formation of impurity phases such as $Bi_2O_{2.75}$, Bi_2O_3 and $Bi_2Fe_4O_9$ [28,29]. Fig. 5 shows the DSC curve of $BiFeO_3$ nanopowder, identifying the two ferroic phase transitions. The endothermic peak at ~370 °C is attributed to the transition from antiferromagnetism to paramagnetism, and the endothermic peak at ~830 °C is ascribed to the ferroelectric-to-paraelectric phase transition. The transition temperatures are basically coincided with previous reports [1–3].

4. Conclusion

In this paper, we describe a polyacrylamide gel route to prepare $BiFeO_3$ nanopowder. It is demonstrated that the present route allows the synthesis of high-purity $BiFeO_3$ nanopowder using EDTA as the chelating agent. On the other hand, the particle morphology can be much improved by adding an appropriate amount of glucose to the precursor solution and adjusting the amount of used acrylamide. The $BiFeO_3$ powder prepared under the optimal conditions is revealed to have a uniform particle size, around 110 nm in average, and the particles are polydisperse without any agglomeration. The

antiferromagnetic and ferroelectric phase transitions are evident from DSC measurements, indicating the multiferroic properties of our $BiFeO_3$ nanoparticles.

Acknowledgments

This work was supported by the Foundation of Gansu Educational Committee (0703B-01) and the Doctoral Research Grant of Lanzhou University of Technology (SB10200701).

References

[1] C. Michel, J.M. Moreau, G.D. Achenbach, R. Gerson, W.J. James, Solid State Commun. 7 (1969) 701–704.
[2] P. Fischer, M. Polomska, I. Sosnowska, M. Szymanksi, J. Phys. C 13 (1980) 1931–1940.
[3] C. Tabares-Munoz, J.P. Rivera, A. Monnier, H. Schmid, Jpn. J. Appl. Phys. Suppl. 24 (1985) 1051–1053.
[4] Y.-H. Lee, J.-M. Wu, C.-H. Lai, Appl. Phys. Lett. 88 (2006) 042903.
[5] D. Lebeugle, D. Colson, A. Forget, M. Viret, Appl. Phys. Lett. 91 (2007) 022907.
[6] J. Wang, J.B. Neaton, H. Zheng, V. Nagarajan, S.B. Ogale, B. Liu, D. Viehland, V. Vaithyanathan, D.G. Schlom, U.V. Waghmare, N.A. Spaldin, K.M. Rabe, M. Wuttig, R. Ramesh, Science 299 (2003) 1719–1722.
[7] T.J. Park, G.C. Papaefthymiou, A.J. Viescas, A.R. Moodenbaugh, S.S. Wong, Nano Lett. 7 (2007) 766–772.
[8] F. Gao, X. Chen, K. Yin, S. Dong, Z. Ren, F. Yuan, T. Yu, Z. Zou, J.-M. Liu, Adv. Mater. 19 (2007) 2889–2892.
[9] C.M. Cho, J.H. Noh, I.-S. Cho, J.-S. An, K.S. Hong, J.Y. Kim, J. Am. Ceram. Soc. 91 (2008) 3753–3755.
[10] C. Chen, J.R. Cheng, S.W. Yu, L.J. Che, Z.Y. Meng, J. Cryst. Growth 291 (2006) 135–139.
[11] S. Shetty, V.R. Palkar, R. Pinto, Pramana J. Phys. 58 (2002) 1027–1030.
[12] N. Das, R. Majumdar, A. Sen, H.S. Maiti, Mater. Lett. 61 (2007) 2100–2104.
[13] S. Farhadi, M. Zaidi, J. Mol. Catal. A: Chem. 299 (2009) 18–25.
[14] S. Ghosh, S. Dasgupta, A. Sen, H.S. Maiti, Mater. Res. Bull. 40 (2005) 2073–2079.
[15] S. Ghosh, S. Dasgupta, A. Sen, H.S. Maiti, J. Am. Ceram. Soc. 88 (5) (2005) 1349–1352.
[16] J. Wei, D.S. Xue, Mater. Res. Bull. 43 (2008) 3368–3373.
[17] J.-H. Xu, H. Ke, D.-C. Jia, W. Wang, Y. Zhou, J. Alloys Compd. (2008), doi:10.1016/j.jallcom.2008.04.090.
[18] A. Sin, P. Odier, Adv. Mater. 12 (2000) 649–652.
[19] G.G. Brand, N. Burford, Advances in Inorganic Chemistry, vol. 50, Elsevier Press, 2000, pp. 285–357.
[20] V. Stavila, A. Gulea, S. Shova, Y.A. Simonov, P. Petrenko, J. Lipkowski, F. Riblet, L. Helm, Inorg. Chim. Acta 357 (2004) 2060–2068.
[21] S.Q. Wu, Y.Y. Liu, L.N. He, F.P. Wang, Mater. Lett. 58 (2004) 2772–2775.
[22] R.M. Silverstein, F.X. Webster, Infrared Spectrometry Spectrometric Identification of Organic Compounds, 6th ed., John Wiley & Sons, Inc., New York, 1996, pp. 71–143.
[23] K. Nakanishi, Infrared Absorption Spectroscopy, Holden Day, San Franciso, 1977.
[24] D. Busch, J. Bailar, J. Am. Chem. Soc. 75 (1953) 4574–4580.
[25] H. Zhang, X. Fu, S. Niu, Q. Xin, J. Alloys Compd. 457 (2008) 61–65.
[26] G.V. Subba Rao, C.N.R. Rao, J.R. Ferraro, Appl. Spectrosc. 24 (1970) 436–445.
[27] W. Kaczmarek, A. Graja, Solid State Commun. 17 (1975) 851–853.
[28] M.M. Kumar, V.R. Palkar, K. Srinivas, S.V. Suryanarayana, Appl. Phys. Lett. 76 (2000) 2764–2766.
[29] I. Sosnowska, T. Peterlin-Neumaier, E. Steichele, J. Phys. C 15 (1982) 4835–4846.